JMEPEG
https://doi.org/10.1007/s11665-021-06437-1

1059-9495/$19.00

Tara Tannins as a Green Sustainable Corrosion Inhibitor for Aluminum

Christian E. Byrne, Oriana D'Alessandro, and Cecilia Deyá

Submitted: 24 October 2020 / Revised: 3 September 2021 / Accepted: 6 November 2021

Tara tannin is studied as an inhibitor of aluminum corrosion, immersed in an aerated and near-neutral NaCl solution and in a wash-primer formulation. Electrochemical tests prove that tara tannins provide good corrosion resistance for aluminum, and scanning electron microscopy coupled to energy dispersive x-ray spectroscopy shows a low formation of corrosion products, absence of Cl and presence of C. These results indicate that tannins act as a mixed-type inhibitor without changing the mechanism of oxygen or aluminum reactions, and that tannin is adsorbed on aluminum surfaces forming a compact hydrophobic barrier that blocks anodic and cathodic areas. A tara tannin primer was formulated and applied on aluminum. Its anticorrosive properties were studied by electrochemical techniques and humidity chamber testing, in which it exhibited an acceptable performance compared with a zinc tetroxychromate primer. Taking into account their less harmful environmental impact, tara tannins are proposed as an alternative to chromates in the formulation of wash-primers.

Keywords aluminum, corrosion, green anticorrosive pigment, tannins, tara, wash-primer

1. Introduction

Due to their distinct properties, aluminum and its alloys are widely used for a wide range of applications including construction, automotive, aviation and aerospace industries, shipbuilding and packaging for food, beverages and pharmaceutical products (Ref 1). In near-neutral solutions (pH interval 4.0-8.5) aluminum exhibits high corrosion resistance due to the formation of a thin and adherent oxide layer on its surface (Ref 2). However, when aluminum is exposed to extreme acidic or alkaline media or to solutions with a high chloride concentration, the oxide film is destroyed and the metal corrodes. In aerated solutions of halides at the passive region of pH, the oxide film experiments localized attacks and breakdowns, and the tendency for aluminum is to corrode non-uniformly by pitting (Ref 3, 4). Several methods have been employed to reduce the corrosion of aluminum and its alloys in different aggressive environments. One of the most common tested methods consists in the application of a coating system (Ref 5-7). A wash-primer is a functional conversion coating deposited onto a metal surface (Ref 8, 9). The main function of a wash-primer is to passivate metallic surfaces to temporarily protect the metals during storage and transportation (Ref 10). These primers must be easily removable and/or must be compatible with the coating scheme that will protect the substrate during its service life. If storage is too long or atmospheric conditions are aggressive, the primer can be damaged, and it must be removed before painting.

Wash-primers are formulated with a corrosion inhibitive pigment and phosphoric acid to phosphatize the metal surface. Hexavalent chromium pigments, like zinc tetroxychromate, are currently the most effective and most frequently employed corrosion inhibitors for aluminum (Ref 11). However, chromates have been questioned due to their toxicity and carcinogenic effects (Ref 12), and different countries have established laws and regulations that tend to limit or restrict their use. This problem has stimulated an active search for alternative and eco-friendly corrosion inhibitors. As a consequence, a large number of organic compounds and natural products have been studied as corrosion inhibitors for aluminum and its alloys (Ref 13). Among these natural products, tannins have been the most widely studied as metal corrosion inhibitors (Ref 14).

Tannins are natural and biodegradable polyphenolic compounds extracted from the bark, fruit and wood of several trees (Ref 15, 16). They have been studied as corrosion inhibitors of steel either in solution or as active pigments in the formulation of protective coatings. The most frequently used have been "quebracho colorado" (*Schinopsis balansae*) (Ref 17), mangrove (*Rhizophora apiculata*) (Ref 18-20), mimosa (black wattle tree, *Acacia mearnsii*) (Ref 21, 22), radiata pine (*Pinus radiata*) (Ref 23, 24), chestnut (*Castanea sativa*) (Ref 25) and tara *(Caesalpinia spinosa)* (Ref 26-30). Tara is a native leguminous tree widely distributed in South America, especially in Peru (Ref 31). Commercial tara powder is a fine light yellow sawdust (100-200 mesh) obtained by triturating the seedless pod, and contains 40-60% w/w tannins (Ref 32). Tannin-rich tara extract is obtained through a process that

Supplementary Information The online version contains supplementary material available at https://doi.org/10.1007/s11665-021-06437-1.

Christian E. Byrne and **Oriana D'Alessandro**, Departamento de Química, Facultad de Ciencias Exactas, Universidad Nacional de La Plata, 47 y 115 s/nº, La Plata, Buenos Aires, Argentina; and CIDEPINT (CICPBA-CONICET-UNLP), Av. 52 e/ 121 y 122, La Plata, Buenos Aires, Argentina; and **Cecilia Deyá**, CIDEPINT (CICPBA-CONICET-UNLP), Av. 52 e/ 121 y 122, La Plata, Buenos Aires, Argentina; and Departamento de Ingeniería Química, Facultad de Ingeniería, Universidad Nacional de La Plata, 1 y 47 s/nº, La Plata, Buenos Aires, Argentina. Contact e-mail: c.deya@cidepint.ing.unlp.edu.ar.

Published online: 22 November 2021

includes solvent extraction (mainly water at 65-70 ºC), filtration, concentration and atomization (Ref 32, 33).

Tara tannins are of the hydrolysable type and are predominantly gallotannins (Fig. 1), which consist of a polygallic acid structure linked by ester unions to quinic acid (Ref 34, 35). Since their extraction does not imply deforestation, tara tannins can be widely used in industry as a green and sustainable raw material (Ref 36). Several authors have studied tannins from various sources as green corrosion inhibitors of aluminum and its alloys. The inhibitive properties of mimosa tannins were tested by exposing different aluminum alloys to different corrosive media (HCl, NaOH and NaCl aqueous solutions) (Ref 37-40). Yahya (Ref 41) investigated the ability of *Rhizophora apiculate* tannins to minimize the corrosion rate of Al alloys in NaCl solutions. Likewise, Nnaji studied the red onion skin tannin (Ref 42) and the cashew nut testa tannin (Ref 43) as corrosion inhibitors of aluminum in HCl solutions. In a recent publication, Byrne (Ref 44) studied the anticorrosive properties of "quebracho colorado" tannins in NaCl solutions and evaluated its use in a wash-primer for aluminum 1050. Hitherto, to the best of our knowledge, there have been no reports in the literature on the use of tara tannins as corrosion inhibitors for aluminum.

The objective of this research was twofold. In the first part, the anticorrosive properties of tara tannins over aluminum immersed in 0.1 M NaCl solutions were studied. In the second part, the tara extract was incorporated in the formulation of a polyvinyl butyral wash-primer, and its anticorrosive performance was evaluated and compared to the correspondent to a classical chromate-based primer.

2. Experimental Section

2.1 Characterization of the Extract

The commercial tara extract Indunor T40 was used, as provided, as the source of tara tannins. According to the provider, to obtain this product, an extraction was performed on the tara powder using a mixture of non-toxic solvents. Then the solvent was recovered, and the product obtained from this extraction was subjected to various purification and concentration processes. Finally, the liquid was atomized, resulting in a fine yellowish powder that is highly soluble in cold water (Ref 45).

The pH of a 0.5 % w/v extract solution (prepared with deionized water) was measured with an Arcano PHS-3E pHmeter.

A Fourier-transform infrared (FTIR) spectrum of the commercial extract was made by preparing a tablet with KBr. The IR spectrometer used was the Spectrum One from PerkinElmer. The scanned wavelength range was between 650 and 4000 cm^{-1}; 12 scans were performed, with a spectral resolution of 4 cm^{-1}.

2.2 Study of Anticorrosive Properties

Electrochemical evaluation of the inhibitory capacity of tara tannins on aluminum was carried out through open circuit potential measurements, the determination of the corrosion current density by means of linear polarization tests, and through the study of potentiodynamic polarization curves. All electrochemical measurements were performed using a Gamry Interface 1000 potentiostat-galvanostat in normally aerated solutions stirred at 300 rpm at room temperature (20 ± 2 °C).

2.2.1 Tannin Extract Concentration Levels. Concentrations between 0.01 and 0.5% w/v of Indunor T40 in 0.1 M NaCl were tested and compared to a blank solution of 0.1 M NaCl without addition of tannin (pH 6.0 ± 0.1). The extract was completely solubilized in these concentrations. Solutions were prepared with deionized water and NaCl p.a. (Biopack).

2.2.2 Substrate Surface Preparation. The substrate used in this research was commercial-purity aluminum with >99.5% Al, denominated aluminum alloy AA1050-H24. The nominal chemical composition is reported in Table 1. In every experiment, a set of three cylindrical rods was employed for each tannin concentration and exposure time. Just before immersion the exposed area was mechanically polished with a series of wet emery papers of variable grades (220, 320, 360 and 600 grit size) and cleaned with ethanol.

2.2.3 Electrochemical Tests. The open circuit potential (E_{OCP}) was measured every 10 min for 5 h using an AA1050 rod of 1.33 cm^2 exposed area and a saturated calomel electrode (SCE) as reference. All the potential values included in this paper were measured employing an SCE.

Linear polarization tests were carried out in a conventional three-electrode electrochemical cell, constituted by an AA1050

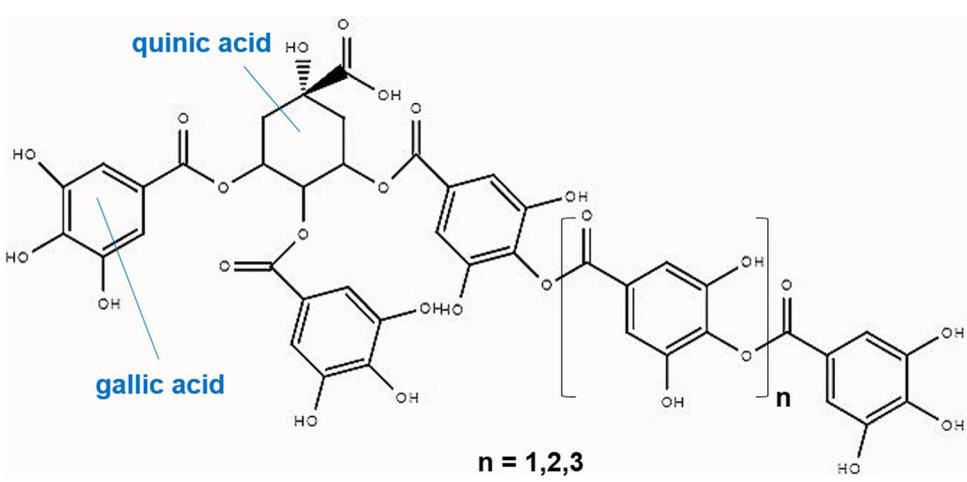

Fig. 1 Main structure of gallotannins in tara

Table 1 Chemical composition of AA1050 (%w/w)

Fe	Si	Cu	Mn	Mg	Cr	Zn	Ti	Al
0.25	0.14	<0.01	0.01	<0.01	<0.01	<0.01	0.01	>99.5

rod of 0.28 cm^2 exposed area as a working electrode, a Pt electrode as a counter electrode and an SCE as reference. The experiments were performed after 5 and 24 h of immersion, selecting a scan range of ± 20 mV from the open circuit potential and a scan rate of 0.25 mV s^{-1}. The corrosion current density (Ic) was calculated using Gamry Echem Analyst Version 6.33 software. Inhibitory efficiency (IE) was calculated according to the following Eq (1):

$$IE(\%) = 100 \cdot (I0 - I)/I0 \quad \text{(Eq 1)}$$

wherein I_0 indicates the Ic of the aluminum immersed in the blank solution, while I is the Ic of the aluminum immersed in each tannin solution at the same time of exposure.

Polarization curves were performed after 5 and 24 h of immersion through a cell similar to the cell described above, using a potential scan range of ± 250 mV from the open circuit potential and a scan rate of 1 mV s^{-1}. From each curve the corrosion potential (E_c), the corrosion current density (I_c) and the cathodic and anodic slopes were obtained by means of the classic Tafel extrapolation method. In E-log I curves, Tafel extrapolation was done employing the least-squares approximation method in the cathodic and anodic branches, taking into account that at Ic = 0, both lines must intersect.

2.2.4 Study of the Exposed Surface by SEM-EDS. AA1050 rods of 1.33 cm^2 exposed areas were immersed in 0.05 and 0.5 % solutions for 5 h and for 24 h. Once that period elapsed, the electrode was rinsed with distilled water and left to dry at 20 ± 2 °C and 70 ± 5% relative humidity. Then, the immersed end of the rod was sawed off and the characteristics of the exposed surface were studied by scanning electron microscopy (SEM). Likewise, its composition was determined by means of energy dispersive X-ray spectroscopy (EDS). The equipment used was a Philips SEM 505 microscope and an EDAX DX PRIME 10 energy dispersive micro-analyzer.

2.3 Formulation, Preparation and Application of an Anticorrosive Primer

A primer based on T40 extract (T40 primer) was developed and its anticorrosive efficiency was compared to a primer containing zinc tetroxychromate (provided by Société Nouvelle des Couleurs Zinciques) as anticorrosive pigment (CR primer) and with another in which the anticorrosive pigment was replaced by talc (TAL primer). The primers were formulated as a two- pack system, A and B, which were stored separately and mixed (4 parts of A and 1 part of B, by weight), before application. Pack A contained the anticorrosive pigment (tara extract or zinc tetroxychromate), the filler (talc), the prime pigment (carbon black), the resin (film-forming material, in this case Butvar® B-76, a thermoplastic polyvinyl butyral resin), the organic solvents to adjust the viscosity (isopropyl alcohol and n-butyl alcohol) and water. The components of pack A were dispersed in a 1 L ball mill for 24 h to achieve a dispersion degree of 5 in the Hegman's gage. Pack B contained isopropyl alcohol, water and phosphoric acid, the last one being essential to provide good adhesion to the substrate. The volume percentages of the components used in the formulation of each pack are detailed in the Supporting Information section, Table S1, and the primers' preparation procedure is summarized in Figure S1. Pigment volume concentration (PVC) values were kept constant to allow for the comparison of the three primers. A commercial AA1050 sheet with 1 mm thickness was cut into coupons with dimensions of 75 mm x 75 mm. The AA1050 coupons were degreased by brushing them vigorously with isopropyl alcohol and were left to dry at 20 ± 2 °C and 70 ± 5% relative humidity. In each coupon a thin primer layer was applied, by brush, up to a dry film thickness of 10 ± 2 μm (5 coupons per primer). The film thickness was measured with a Schwyz SC117-02 Coating Thickness Gauge. The coated coupons (called T40, CR or TAL, according to the primer used) were then allowed to cure for 5 days at 20 ± 2 °C and 70 ± 5% relative humidity. The coated coupons were tested together with a series of degreased coupons not subjected to any painting treatment (blank coupons, B). The edges of the coupons were protected with blue vinyl duct tape (Brand 3M, model 3903).

2.4 Evaluation of the Coated Coupons

2.4.1 Electrochemical Evaluation. The coated coupons were electrochemically characterized by open circuit potential (E_{OCP}) measurements, conductivity measurements to determine ionic resistance (Ri), and by linear polarization tests to determine polarization resistance (Rp). The electrochemical tests were performed in cells constructed by delimiting a circular area of 3 cm^2 on the coated surface using a polyvinyl chloride tube. Each tube was adhered to the panel with epoxy type glue and then sealed with beeswax on the outside. Finally, a defined volume of 0.1 M NaCl was added as electrolyte. For each type of coated coupons, the determinations were carried out in triplicates after different times of exposure to the chloride solution.

The E_{OCP} measurements were performed with a Gamry Interface 1000 instrument, and an SCE was used as reference.

Ionic resistance between the coated substrate and a Pt electrode was calculated through conductivity (Ci) measurements with an ATI Orion Model 170 conductivity meter at 1000 Hz, according to the following Eq (2):

$$Ri(\Omega \cdot cm^2) = [1/Ci(\mu S)] \cdot 3\ cm^2 \cdot 106 \quad \text{(Eq 2)}$$

Linear polarization tests (without IR compensation) were carried out with a Gamry Interface 1000 potentiostat-galvanostat, employing a typical three-electrode cell, with a Pt counter electrode and SCE as reference. The selected scan range was of ± 20 mV from the open circuit potential, and the scan rate was of 1 mV s^{-1}. Polarization resistance (Rp) was calculated using the Gamry Echem Analyst Version 6.33 software. The employment of this technique was justified by the low ionic resistance of the primer film (Ref 46, 47).

2.4.2 Humidity Chamber Exposure. A set of coated coupons (4 per primer) was placed in a humidity chamber (100% relative humidity and 38°C, ASTM D 2247) (Ref 48). Visual observation of samples was made after 4, 8 and 14 days of exposure to evaluate adhesion (adhesion by tape test, ASTM D 3359) (Ref 49), the degree of blistering (ASTM D 714) (Ref 50) and the eventual presence of corrosion. For the last, the scale of visual classification of aluminum corrosion specified in Table 2 was used (Ref 51).

2.4.3 Evaluation of the Underlying Substrate by SEM-EDS. After humidity chamber exposure, the primer coat was removed mechanically from each coupon by a lab spatula, and the surface of the underlying aluminum substrate was analyzed by SEM-EDS. The equipment used was an FEI Microscope Quanta 200 model and an EDAX energy dispersive micro-analyzer with an Apollo 40 detector.

3. Results and Discussion

3.1 Characterization of the Extract

According to the manufacturer, the tara extract Indunor T40 contains 90% w/w of tannins, 7% w/w of moisture and 0.4% (w/w) of total ash.

The pH value of a 0.5% w/v extract solution was 5.0.

The FTIR spectrum of the T40 tara tannins extract is shown in Fig. 2. The assignment of each band and its characteristics as markers in tannins' identification are summarized in Table 3 (Ref 52-54). Bands at 757 and 869 cm^{-1} are due to the aromatic C-H out-of-plane bending while the one at 1089 cm^{-1} is due to C-H in-plane-bending. Bands at 1024, 1195 and 1317 cm^{-1} correspond to C-O and the band at 1700 cm^{-1} corresponds to C=O stretching vibration. Aromatic ring bands can be seen at 1445, 1540 and 1610 cm^{-1}. The broad band at 3000-3700 cm^{-1} is due to OH stretching, characteristic of the polyphenolic compounds (Ref 52-54).

3.2 Study of Anticorrosive Properties

3.2.1 Open Circuit Potential Measurements. Figure 3 shows the E_{OCP}—time diagrams corresponding to aluminum samples exposed to 0.1 M NaCl solutions with and without tara tannins extract addition. As can be observed in this figure, two clearly defined zones are present: a transient zone, where E_{OCP} evolves from an initial potential to a steady-state potential, which defines the second zone. In the transient zone, the potential shifts to more positive values over time due to the generation of a passive film formed with sparingly soluble aluminum corrosion products, such as oxides, hydroxides and oxyhydroxides (Ref 55, 56). The formation of the passive film over the surface is faster when the samples are exposed to the blank solution (electrolyte without tannin), and the steady-state potential is reached sooner. When the tara tannins extract is added to the aggressive medium, the corrosion reactions are repressed, and consequently the film develops more slowly (Ref 57). This effect is more marked in the 0.5% solution, which is the last to reach the steady-state.

It can also be noted that the steady-state E_{OCP} shifts to more noble values as the tara tannin concentration increases: − 664, − 659, − 659, − 649, − 644 and − 640 mV for the 0, 0.01, 0.05, 0.1, 0.3 and 0.5% solutions, respectively. This is indicative that the addition of tara tannins modify the structural characteristics and/or the physicochemical properties of the film, making it more stable, therefore achieving a less reactive aluminum surface.

3.2.2 Linear Polarization Curves. The corrosion current density Ic and the inhibitory efficiency IE of the aluminum samples immersed for 5 and 24 h in the tara extract solutions are shown in Table 4. It can be noted that after 5 h of immersion in tannin extract solutions, there is a significant decrease in the corrosion reaction rate of the aluminum samples, achieving IE values close to 96%. As will be discussed in more detail in the next section, when the tara extract is added to the aggressive medium, the tannin molecules are adsorbed onto the aluminum surface, and many reaction sites are blocked, decreasing the intensity of the corrosion reactions (Ref 40). The value of inhibitory efficiency indicates the adsorption ability of inhibitor molecules on the metal surface; the higher adsorption results in a higher IE (Ref 58).

After 24 h of immersion, the 0.5% solution retained 96% IE, while for the lower concentration solutions, the IE decreased to values of around 84%. The lower IE in these last conditions could be caused by desorption of inhibitor molecules due to changes in the physicochemical properties of the protective layer (Ref 58-60) and/or to the partial solubilization of tannin-metal complexes (Ref 61, 62). Consequently, fewer tannin molecules are adsorbed and more reaction sites remain exposed, which leads to a higher rate of reaction. These adsorption difficulties are evidently not significant in the more concentrated solution (more molecules are available to bind at adsorption sites), so its performance remains unaltered.

The inhibition efficiency values, obtained with tara tannins, are similar to those obtained employing red onion skin, cashew nut testa, *Acacia mearnsii* or *"Quebracho colorado"* tannins for almost pure aluminum alloys (AA1XXX) in different media (Ref 40, 42-44).

3.2.3 Potentiodynamic Polarization Curves. Potentiodynamic polarization curves for AA1050 samples immersed 5 h in 0.1 M NaCl solutions with 0, 0.05 and 0.5% tara tannin

Table 2 Scale of visual classification of aluminum corrosion

Classification	Description
No appreciable attack (N)	There is no appreciable attack; the surface may be discolored
Pitting (P)	Discrete pits
Filiform (F)	Appearance of corrosion filaments
General (G)	Fairly uniform corrosion with accumulation of dusty corrosion products
Exfoliation (E)	Visible separation of metal in layers

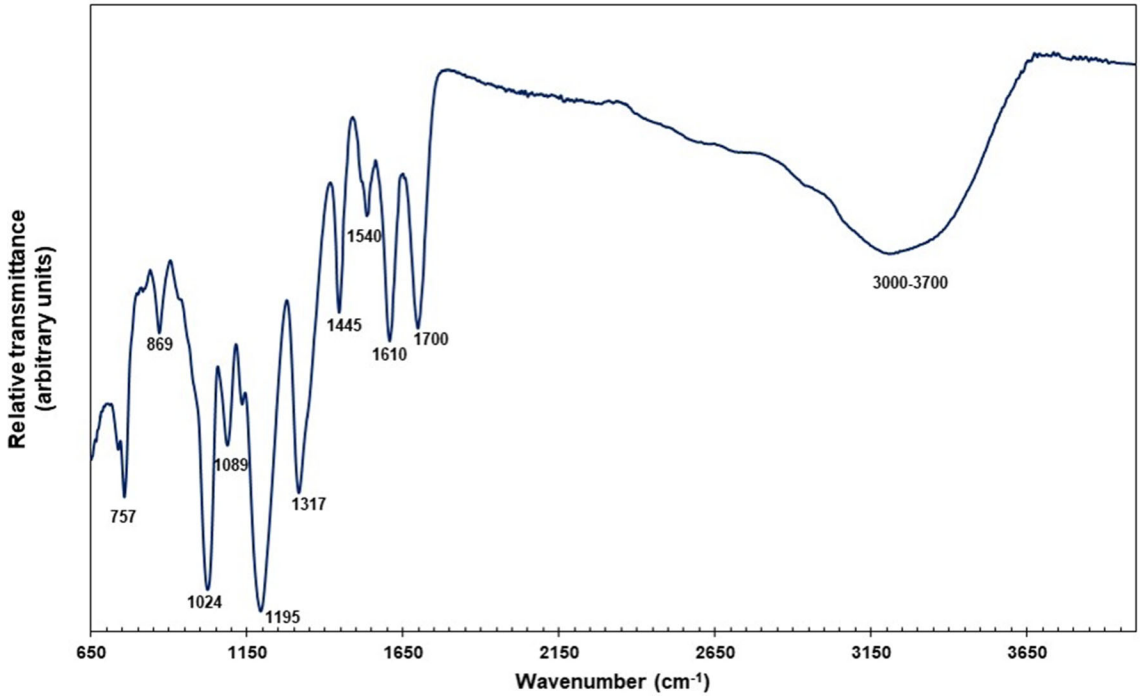

Fig. 2 FTIR spectrum of the T40 tara tannins extract

extract can be seen in Fig. 4. Only selected concentrations were studied as the results in the previous assays were similar. For a better visualization, log I is represented as a function of the overpotential η, which was calculated as the difference between the working electrode potential E and the corrosion potential Ec obtained by the extrapolation method:

$$\eta = E - Ec \quad \text{(Eq 3)}$$

Taking as reference the 0.1 M NaCl solution without extract (blank solution), the current density decreases in both cathodic and anodic branches, with a more marked effect on the 0.5 % solution. This mixed inhibition is consistent with the mechanism of adsorption and film formation that is characteristic of many organic inhibitors, where a compact hydrophobic barrier is formed on the surface, blocking anodic and cathodic areas (Ref 63, 64). The efficiency of these organic inhibitors has been associated with the presence of heteroatoms (N, S, O and P) or π-electrons, which serve as adsorption centers. Tannin molecules can retard corrosion reactions by adsorbing on metal surfaces (Ref 65). Several authors (Ref 39, 40) have pointed out that the adsorption of tannin molecules may occur via the high electronic densities of the oxygen lone pairs in hydroxyl groups and of the π-system of the aromatic rings, forming an adsorption layer on the metal surface.

In NaCl solutions, the anodic reaction is the dissolution of aluminum catalyzed by Cl^- ions (Ref 66). The aluminum dissolution is an activation-controlled process. However, at high anodic overpotential, a limit diffusion current appears due to the transport of chloride ions from the solution to the metal surface through the oxide film. Chloride ions play a crucial role in the anodic dissolution process of aluminum. These anions not only compensate the charge of the Al^{3+} cations generated in the anodic reaction, but they also actively intervene in a process of destabilization of the oxide passive film that leads to pitting. According to the literature (Ref 13, 67-70), the mechanism of destabilization of the oxide film by Cl^- would occur as follows: (i) in near-neutral solutions the oxide/solution interface (an oxyhydroxide type material) has a net positive charge and so chloride anions are electrostatically attracted to the surface; (ii) Cl^- is adsorbed on the oxide surface; (iii) Cl^- is incorporated into the bulk of the oxide; (iv) Cl^- moves into the oxide film; (v) weakening the Al-O bonds and forming soluble aluminum chloride (Al-Cl) and oxychloride (O-Al-Cl) complexes; (vi) the oxide film becomes thinner and breaks down; (vii) localized Cl^--assisted dissolution of aluminum at the metal/oxide interface in consecutive one-electron transfer reactions takes place; (viii) and blisters, cracks and pits are formed (Fig. 5a).

In near-neutral aerated solutions, the cathodic reaction is dominated by the diffusion and the reduction of dissolved oxygen (Ref 69, 71). The presence of the organic film restricts the diffusion of oxygen and, in consequence, slows down the cathodic reaction. According to Fig. 4, this restriction is more effective in the more concentrated tannin solution.

In tara extract solutions, tannin molecules are adsorbed and form a stable organic layer onto aluminum, which interferes with both the adsorption of Cl^- ions and the diffusion of Al (III) soluble complexes from the oxide surface to the bulk solution (Ref 32). In addition, the adsorption of tannin molecules on the aluminum surface removes or depletes some of the water molecules originally adsorbed onto the surface, which blocks the formation of hydrated/hydroxylated intermediate species during the aluminum dissolution (Ref 64). Consequently, the tannin addition inhibits the anodic metal dissolution reaction, and corrosion is retarded (Fig. 5b). Again, this inhibitory effect is more marked in the more concentrated tannin solution.

Figure 6 shows the potentiodynamic polarization curves for AA1050 samples immersed for 24 h in 0.1 M NaCl solutions with 0, 0.05 and 0.5% tara tannin extract. It can be observed that after 24 h of immersion the 0.05% extract addition has almost no effect on the cathodic process but still reduces the

Table 3 Assignments and characteristics of the FTIR bands in the T40 tara extract

Band (cm^{-1})	Assignment	Comments
1024	Stretch vibrations of C-O bonds	Characteristic common bands present in tannins from different vegetable sources
1195		
1445	Aromatic ring stretch vibrations	
1540		
1610		
1317	Symmetric stretching of the C-O bond of the ester function	Characteristic common bands present in hydrolysable tannins
1700	Stretching vibration of the carbonyl function (C=O)	
757	Aromatic C-H out-of-plane bending	Characteristic bands of gallotannins
869		
1089	Aromatic C-H in-plane bending	
3000-3700	Sum of the –OH stretching derived from different chemical environments	Characteristic of polyphenolic extracts

anodic current considerably. The organic film formed in these conditions does not delay the oxygen diffusion but interferes with the chloride adsorption and the successive aluminum dissolution. According to Rahim (Ref 72) this fact could be attributed to differences in film thickness: thick surface layers having poor electronic-conductive properties can restrict the diffusion of oxygen, but thin passivating films usually inhibit only the anodic metal dissolution reaction. This situation leads to a higher Ic and consequently a lower IE compared to the one obtained after 5 h of immersion, which is in agreement with the previous results observed in the linear polarization studies. The current density of the samples immersed for 24 h in the 0.5% extract solution exhibited a meaningful decrease in both cathodic and anodic branches, so it can be concluded that in this condition the passive film is thicker and retains its oxygen diffusion blocking properties.

Electrochemical parameters, namely corrosion potential (Ec), corrosion current density (Ic), cathodic slope and anodic slope were calculated from the curves of Fig. 4 and 6 and are summarized in Table 5. The open circuit potential (E_{OCP}) measured prior to polarization is also tabulated.

A shift of Tafel Ec to more positive values from E_{OCP} is observed. This shift is generally observed in the polarization curves obtained by negative scan at low and medium scan rate, and could be attributed to the disturbance of the charging current (Ref 44, 73, 74). However, the Ec trend is similar to that of the E_{OCP}: a shift toward more anodic values when tara tannins are added. This ennoblement of the corrosion potential suggests that, despite behaving like mixed-type inhibitors, in these experimental conditions tara tannins preferentially inhibited the anodic reaction. This mixed-type inhibition with predominantly anodic effectiveness was also noticed by Adam (Ref 59) with mild steel substrates exposed to mimosa, chestnut and mangrove tannins.

The Ic values obtained by the Tafel extrapolation method were located in the same range as those obtained previously by the linear polarization tests. The anodic Tafel slopes were estimated by the least-squares approximation method, using polarization data with η between +10 to $\approx$+50 mV in the anodic curves (Fig 4 and 6). The diffusion-controlled cathodic slopes were calculated similarly, using data with η between 100 and − 150 mV in the cathodic curves. It can be observed that the values of cathodic and anodic slopes did not change significantly; indicating that tara extract addition to NaCl solutions does not change the mechanism of oxygen reduction or aluminum dissolution reactions. This confirms that the inhibitor molecules are adsorbed on the aluminum surface and simply block the available metal surface area.

3.2.4 Study of the Exposed Surface by SEM-EDS. SEM micrographs shown in Fig. 7a present the surface of not exposed AA1050. As can be seen in this figure, the surface was covered by sanding scratches formed during the polishing treatment. Besides Al, a little amount of O is present (Table 6).

Figure 7(b)-(d) display SEM micrographs of the AA1050 electrode exposed surfaces after 5 h of immersion in naturally aerated 0.1M NaCl solutions with 0, 0.05 and 0.5% tara tannin extract, respectively. Their respective compositions as determined by EDS analysis are summarized in Table 6.

In the sample exposed to the blank solution (Fig. 7b), the sanding scratches were barely visible due to the extensive accumulation of corrosion products rich in oxygen, as suggested by the high O content detected (Al/O ratio = 2.1).

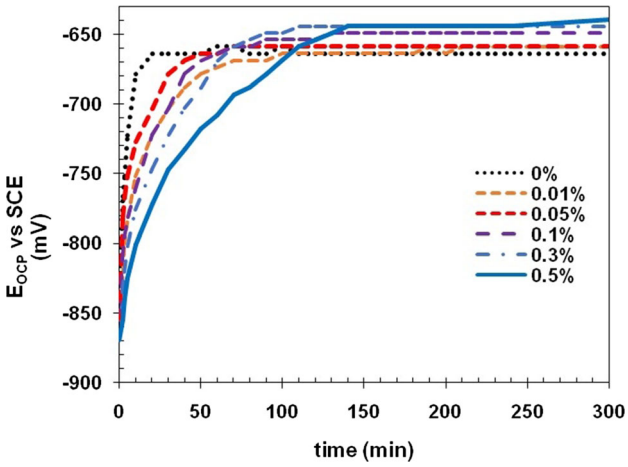

Fig. 3 Open circuit potential (E_{OCP})vs. time for the AA1050 alloy immersed 5 h in 0.1 M NaCl

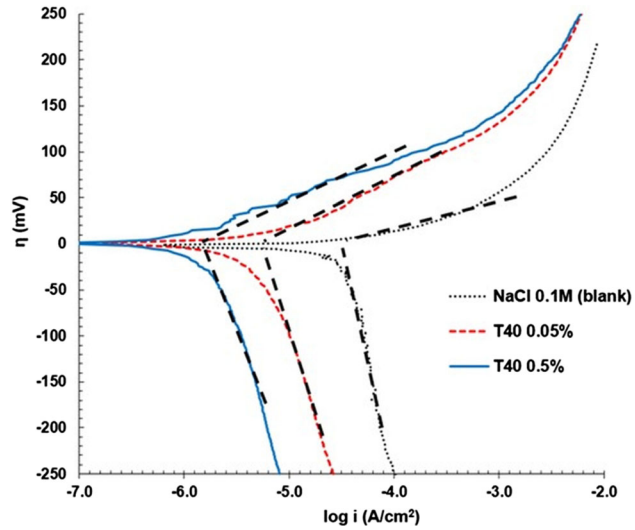

Fig. 4 Potentiodynamic polarization curves for AA1050 immersed 5 h in 0.1 M NaCl with 0 (blank), 0.05 and 0.5% tara tannins extract

Table 4 Corrosion current density and inhibition efficiency obtained from the linear polarization experiments (mean value ± SD)

	Ic (μA/cm^2)		IE (%)	
	Time (h)		Time (h)	
T40 extract concentration (%w/v)	**5**	**24**	**5**	**24**
0	61±1	43 ± 2		
0.01	2.9 ± 0.6	8.3 ± 2.0	95 ± 2	81 ± 3
0.05	2.4 ± 0.6	8.3 ± 2.0	96 ±2	81 ± 3
0.10	3.1 ± 0.2	7.0 ± 1.0	95 ± 2	84 ± 3
0.30	2.8 ± 0.6	5.1 ± 1.0	95 ± 2	88 ± 3
0.50	2.3 ± 0.6	1.5 ± 0.3	96 ± 2	97 ± 3

Incipient pits and fine particles with colloidal dimensions that show a strong tendency toward agglomeration can also be observed. EDS analysis demonstrated the presence of chlorine on the surface, indicating the existence of chloride anions either adsorbed or incorporated into the structure of the oxide film (Fig. 5a). In the AA1050 immersed in 0.05% tannin solution (Fig. 7c), SEM examination revealed the presence of small amounts of corrosion products, but the sanding scratches were still clearly visible. The EDS analysis shows that the surface had a higher Al/O ratio (7.2) compared to the one immersed in the blank solution, indicating a smaller amount of corrosion products, due to the lower corrosion rate in the presence of tannins. Moreover, the presence of C was detected, indicating the formation of a protective film of an organic nature. Finally, no chlorine was present within EDS resolution limits, indicating that a high blocking capacity of chloride adsorption can be achieved by this protective layer.

The micrographs of the aluminum sample immersed in the 0.5 % tannin solution (Fig. 7d) show a more homogeneous surface, with hardly any presence of corrosion products and with the sanding scratches partially covered. The Al/O ratio (6.8) is also higher than the one immersed in the blank solution, and similar to that of the 0.05% tannin solution. EDS analysis demonstrated the presence of C and lack of chlorine, indicating the high blocking capacity of the organic layer.

Figure 8(a)-(c) and Table 6 show SEM micrographs of the aluminum samples' exposed surfaces after 24 h of immersion in the tested solutions and their respective compositions as determined by EDS analysis. In the sample immersed in the NaCl solution without tannin addition (Fig. 8a), the presence of pits, cracks and a large accumulation of corrosion products with globular structure can be observed. EDS analysis reveals again a low Al/O ratio (2.5) and the presence of chlorine on the surface. SEM images of the aluminum samples immersed for 24 h in both NaCl solutions with tara extract (Fig. 8b and c, 0.05% and 0.5%, respectively) show the presence of incipient pits, cracks and some areas covered with corrosion products. EDS analysis reveals the presence of C and the absence of chlorine, indicating the formation of organic films that retain their inhibitory action on chloride adsorption after a 24 h exposure, which is in agreement with that suggested previously in the potentiodynamic polarization curves. Finally, it can be verified that the Al/O ratio is also high for the samples immersed in the tannin solutions (with a slightly higher value for the more concentrated solution), indicating less formation of

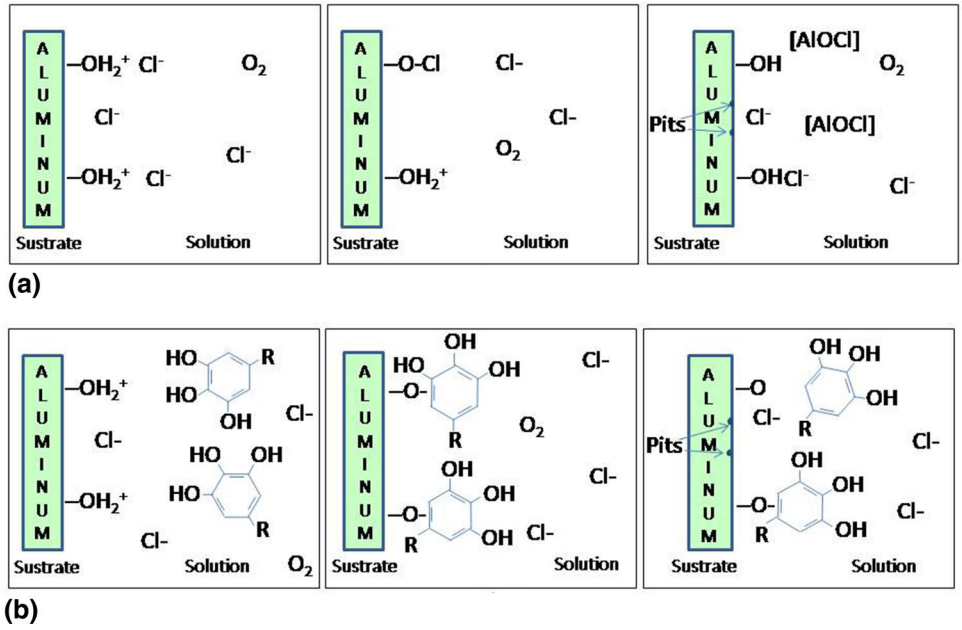

Fig. 5 Scheme of Al in Cl^- media, (a) corrosion, (b) protection by tannin

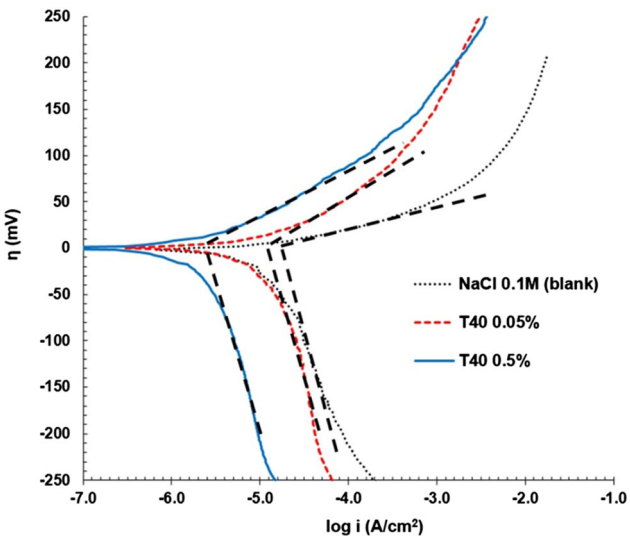

Fig. 6 Potentiodynamic polarization curves for AA1050 immersed 24 h in 0.1 M NaCl with 0 (blank), 0.05 and 0.5% tara tannins extract

corrosion products and proving once again that the presence of tara tannins leads to a decrease in the corrosion rate.

The mean integration errors of the peaks of the elements are: C: 4.8, O: 2.0, Al: 0.3, Cl: 4.4, Fe: 5.2, being higher when the amount of element is small.

3.3 Evaluation of the Coated Coupon

3.3.1 Electrochemical Evaluation. Figure 9 shows the time-dependent response of the open circuit potential (E_{OCP}) for bare and coated AA1050 substrates. T40 showed a continuous ennoblement of the E_{OCP} values, ranging from 650 mV at the first measurements to − 445 mV at the end of the experiment. CR showed the least negative potentials during the first 100 h, but then the E_{OCP} descended to values ≈100 mV below those of T40. The uncoated aluminum showed the most negative Ec, with values more negative than − 800 mV during the first 4 h and in the range of − 700 to − 800 mV during the remainder of the assay . During the first 24 h TAL showed open circuit potentials close to those of T40, but then E_{OCP} became more negative, with values in the same range of the bare aluminum. In conclusion, it can be

Table 5 Electrochemical parameters obtained from potentiodynamic polarization curves

Immersion time	T40 extract concentration, %w/v	E_{OCP}, mV vs SCE	Ec, mV vs SCE	Ic, μA/cm²	Cathodic slope, mV/decade	Anodic slope, mV/decade
5 h	0	− 664	− 629	20	− 311	32
	0.05	− 659	− 612	7	− 370	56
	0.5	− 640	− 600	2	− 356	49
24 h	0	− 664	− 648	55	− 316	24
	0.05	− 644	− 608	18	− 445	68
	0.5	− 638	− 606	3	− 336	55

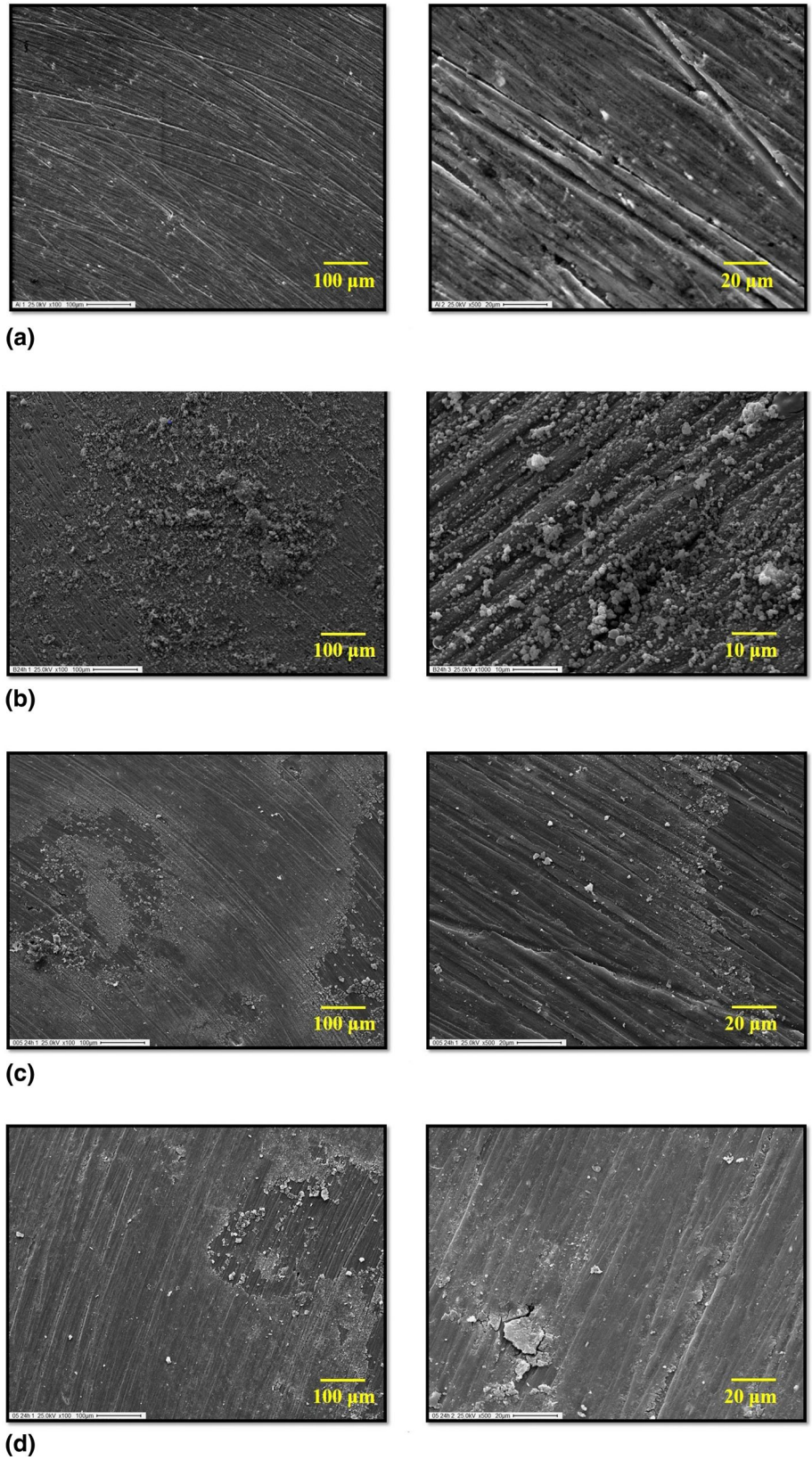

Fig. 7 SEM micrographs of AA1050 (a) not exposed, after 5 h of immersion in 0.1M NaCl (b) without tara tannins, (c) with 0.05% T40 tara extract, (d) with 0.5% T40 tara extract

Table 6 EDS analysis of the 5 h and 24 h immersed aluminum samples

Samples		% w/w				
		Al	O	Fe	C	Cl
Not exposed AA 1050		96.70	2.98	0.32	…	…
5 h exposed	Blank	66.21	31.80	0.69	…	1.30
	T40 0.05%	67.56	9.43	0.61	22.40	…
	T40 0.5%	79.49	11.75	0.67	8.09	…
24 h exposed	Blank	70.22	28.22	0.71	…	0.85
	T40 0.05%	70.49	9.78	0.72	19.01	…
	T40 0.5%	76.23	9.67	1.01	13.09	…

highlighted that the coupons covered with the tara tannin primer showed the noblest E_{OCP} values beyond 100 h of exposure to the chloride medium, which suggests the presence of a less reactive aluminum surface.

In Fig. 10, it can be observed that the ionic resistance (Ri) values for T40 and CR increased from the beginning of the experiment to the first 50 h, achieving a maximum of $6.5 \cdot 10^4$ and $8.5 \cdot 10^4$ $\Omega \cdot cm^2$, respectively. Then, Ri progressively decreased to levels around $1 \cdot 10^4$ $\Omega \cdot cm^2$ at 300 h. For TAL Ri was around $1 \cdot 10^4$ $\Omega \cdot cm^2$ throughout the experiment. In the case of uncoated AA1050, added as a comparison, Ri values were lower than $4 \cdot 10^2$ $\Omega \cdot cm^2$. The ionic resistance of coated samples is related to the penetration of water and electrolytes through the coating film over time. These Ri values on the order of 10^4 $\Omega \cdot cm^2$ are low and indicate a poor barrier effect. This failure occurs when a wash-primer coat is applied alone, as it is permeable to water and electrolytes over long periods of exposure.

Polarization resistance (Rp) measurements provide information about the corrosion rate of a coated substrate. Once the water permeates through the coating, the active pigments dissolve continuously, limiting the electrochemical corrosion processes at the coating-metal interface (and thus increasing Rp). Figure 11 displays the Rp values of the coated coupons as a function of the exposure time to the NaCl solution.

The Rp values for T40 increased abruptly during the first 24 h of the experiment, from $\approx 1 \cdot 10^5$ to $2.5 \cdot 10^6$ $\Omega \cdot cm^2$. Then, the values increased more slowly, being between $3 \cdot 10^6$ and $9 \cdot 10^6$ $\Omega \cdot cm^2$ up to the end of the experiment. CR exhibited Rp values of $\approx 1 \cdot 10^7$ $\Omega \cdot cm^2$ for all measurements. TAL Rp values also increased during the first 72 h, remaining near or even below B (uncoated coupons) values. Afterward, TAL Rp values were among those of T40 and B, around $1\text{-}3 \cdot 10^6$ $\Omega \cdot cm^2$. Regarding B, Rp values increased from $5 \cdot 10^4$ to $2 \cdot 10^6$ $\Omega \cdot cm^2$ during the first 72 h, but then slowly decreased. It can therefore be concluded that although CR always had the highest Rp values, T40 had acceptable Rp values after 24 h of exposure to the chloride solution, and they were even within close range of CR values after 240 h. These relations can be clearly observed in the linear polarization curves for the coated coupons after 24 and 240 h of exposure, which are plotted in Figures S2 and S3 in the Supporting Information section.

3.3.2 Humidity Chamber Exposure. Table 7 summarizes the adhesion grade and the visual evaluation results of the coated coupons after different exposure times in the humidity chamber. At the beginning of the test, the adhesion of the primers to the aluminum substrate was good in every case, with a 4B qualification (Table 7). However, the adhesion of the systems exhibited a gradual loss as time elapsed. The T40 primer exhibited an adhesion performance similar to that of the CR control: regular (3B) after 4 days in the chamber and poor (2B) after 8 and 14 days. In the case of the TAL primer, nevertheless, the adhesion was completely lost after 4 days in the chamber. The aluminum coupons without a primer (B) were almost completely covered with corrosion products after 4 days in the chamber (Table7, Figure S4 a) in the Supporting Information section). T40 and CR showed no appreciable attack after 14 days in the chamber (Figures S4 b and c), while TAL showed pitting after 8 days and general corrosion after 14 days of exposure, (Figure S4 d). None of the samples showed the formation of blisters along the assay.

Similar results were obtained employing "quebracho" tannin as anticorrosive pigments in wash-primers (Ref 44).

3.3.3 Evaluation of the Underlying Substrate by SEM-EDS. The surface morphology of the coupons' underlying substrate after humidity chamber exposure can be observed in the SEM micrographs in Fig. 12. Likewise, the data corresponding to the EDS analysis of the surfaces are reported in Table S2.

The surface of the uncoated aluminum (B) showed extensive accumulation of oxygen-rich corrosion products, arranged as colloidal particles grouped into agglomerates (Fig. 12 a, Table S2). The underlying aluminum in T40 showed a rather homogeneous surface with some areas of slight deposit of corrosion products (Fig. 12b). The Al/O ratio (11.7) increased considerably, compared to the uncoated aluminum (Al/O = 1.4), indicating a lower formation of corrosion products and thereby a decrease in the corrosion rate. The EDS analysis also showed the presence of C (from the resin, the tannins or the carbon black) and P (from the phosphoric acid), indicating a good adhesion of the primer to the aluminum surface. In the case of CR, the primer could not be completely removed. The underlying aluminum surface showed a uniform aspect (Fig. 12c) with the presence of C, denoting good adhesion, but no evidence of P (Table S2). The extremely high Al/O ratio (48.4) demonstrates an excellent anticorrosive performance. As in T40, the aluminum surface in TAL revealed zones with accumulation of corrosion products (Fig. 12d). However, the lower Al/O ratio (2.7) indicates an increased corrosion rate. The detection of C and P also denotes good adhesion.

Given their acceptable performance in the electrochemical and humidity chamber exposure tests, and fundamentally taking into account their less harmful environmental impact, tara tannins can be proposed as a non-polluting, inexpensive and eco-friendly alternative to chromates in the formulation of wash-primers for temporary aluminum protection.

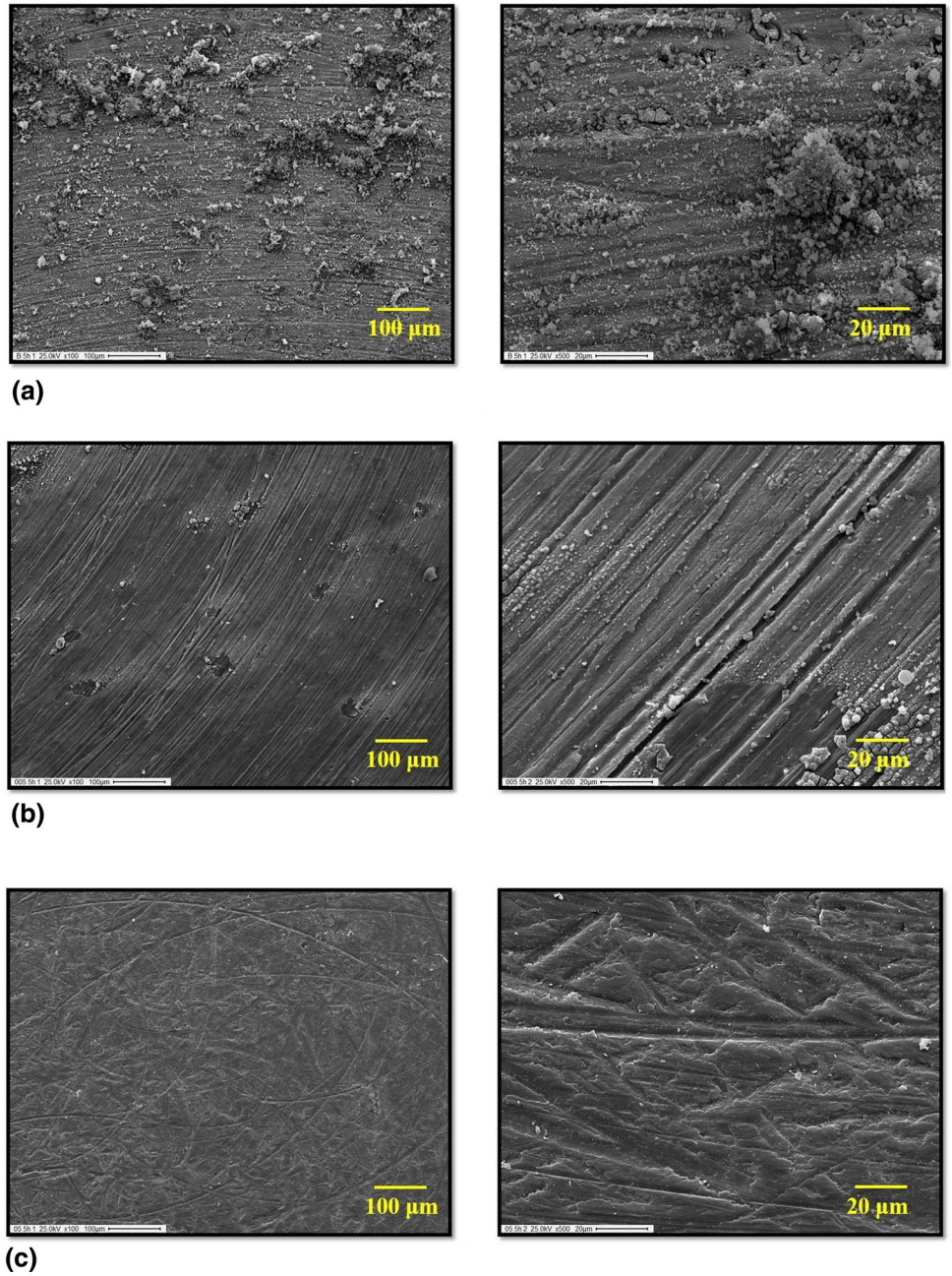

Fig. 8 SEM micrographs of AA1050 after 24 h of immersion in 0.1M NaCl (a) without tara tannins, (b) with 0.05% T40 tara extract, (c) with 0.5% T40 tara extract

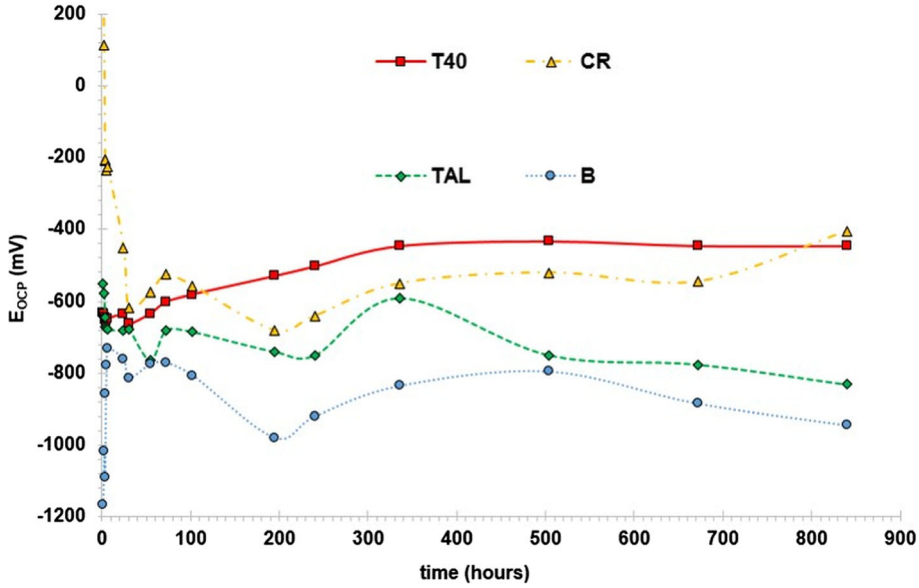

Fig. 9 Open circuit potential (E_{OCP}) as a function of time for bare and coated AA1050 substrates

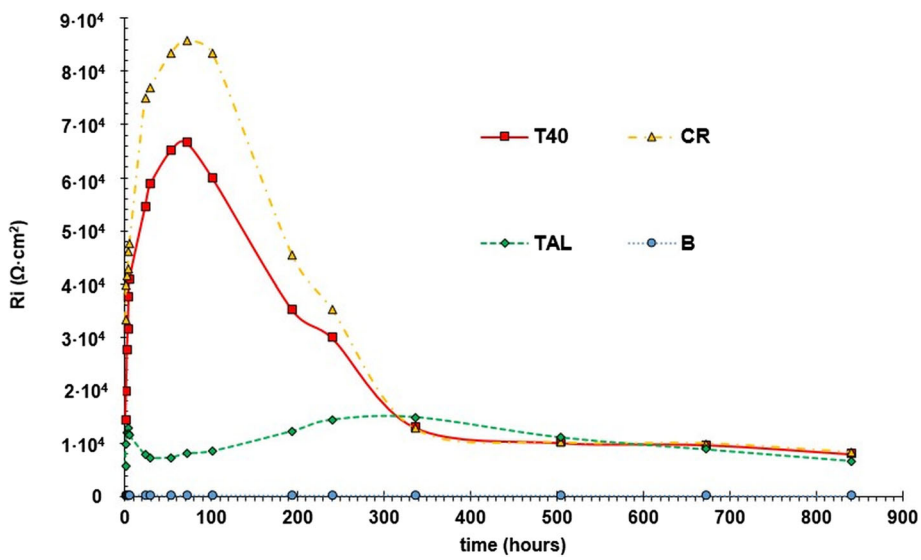

Fig. 10 Ionic resistance values (Ri) as a function of time for coated coupons

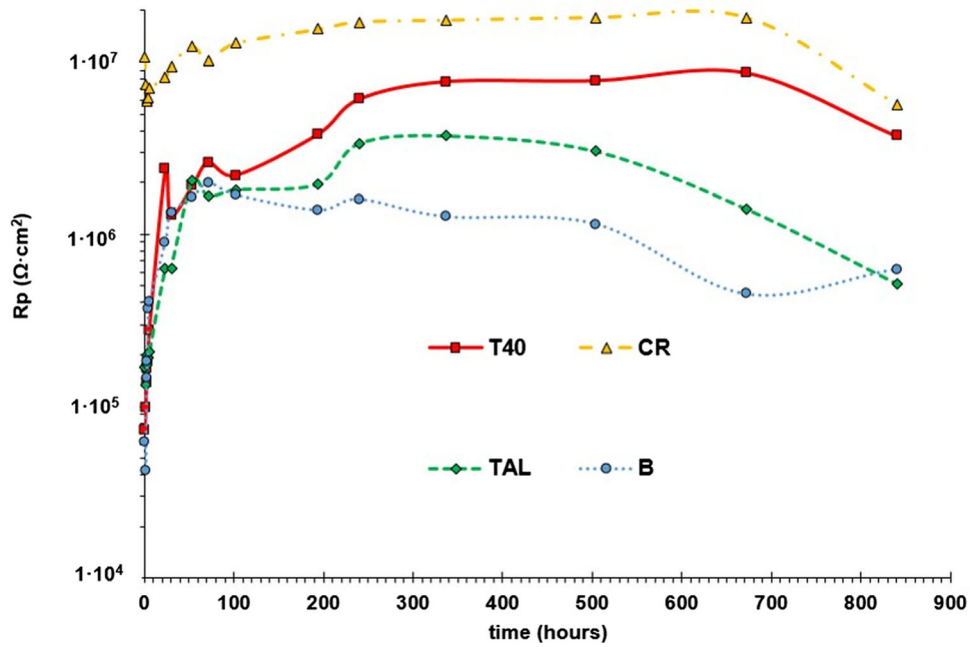

Fig. 11 Polarization resistance values (Rp) as a function of time for coated coupons

Table 7 Adhesion grade and visual evaluation results of the coated coupons after different exposure times in the humidity chamber

	Adhesion grade (ASTM D 3359)*				Classification of corrosion**		
	Time (days)				Time (days)		
Coated coupons	**0**	**4**	**8**	**14**	**4**	**8**	**14**
B	…	…	…	…	G	G	G
T40	4B	3B	2B	2B	N	N	N
CR	4B	3B	2B	2B	N	N	N
TAL	4B	0B	0B	0B	N	P	G

*5B: 0% area removed 4B: 0-5% 3B: 5-15% 2B: 15-35% 1B: 35-65% 0B: >65%
**N: No appreciable attack; P: Pitting; F: Filiform; G: General; E: Exfoliation

4. Conclusions

Tara tannins have proven to be efficient corrosion inhibitors for aluminum in naturally aerated near-neutral NaCl solutions. These tannins have acted as mixed inhibitors, decreasing cathodic and anodic currents in potentiodynamic polarization curves. In these plots, cathodic and anodic slopes values did not change significantly, indicating that tara extract addition to NaCl solutions does not change the mechanism of oxygen reduction or aluminum dissolution reactions. This suggests that tannin molecules are adsorbed on the aluminum surface and form a compact hydrophobic barrier that simply blocks anodic and cathodic areas. In the presence of tannins, SEM-EDS analysis has demonstrated lower formation of corrosion products, the absence of Cl and the presence of C, indicating the formation of a protective film of an organic nature with a high chloride adsorption blocking capacity.

Tara tannins can be incorporated in the formulation of primers for aluminum substrates. Their effectiveness in the corrosion protection of aluminum was determined by means of electrochemical techniques and humidity chamber testing, showing an acceptable performance as compared to a classical zinc tetroxychromate primer. Taking into account the laws and regulations that tend to limit or restrict the use of Cr (VI) compounds due to their harmful environmental impact and highlighting the fact that tara tannin extraction does not imply deforestation (as they are present in the fruits of the tree), these tannins are proposed as a non-polluting, sustainable, inexpen-

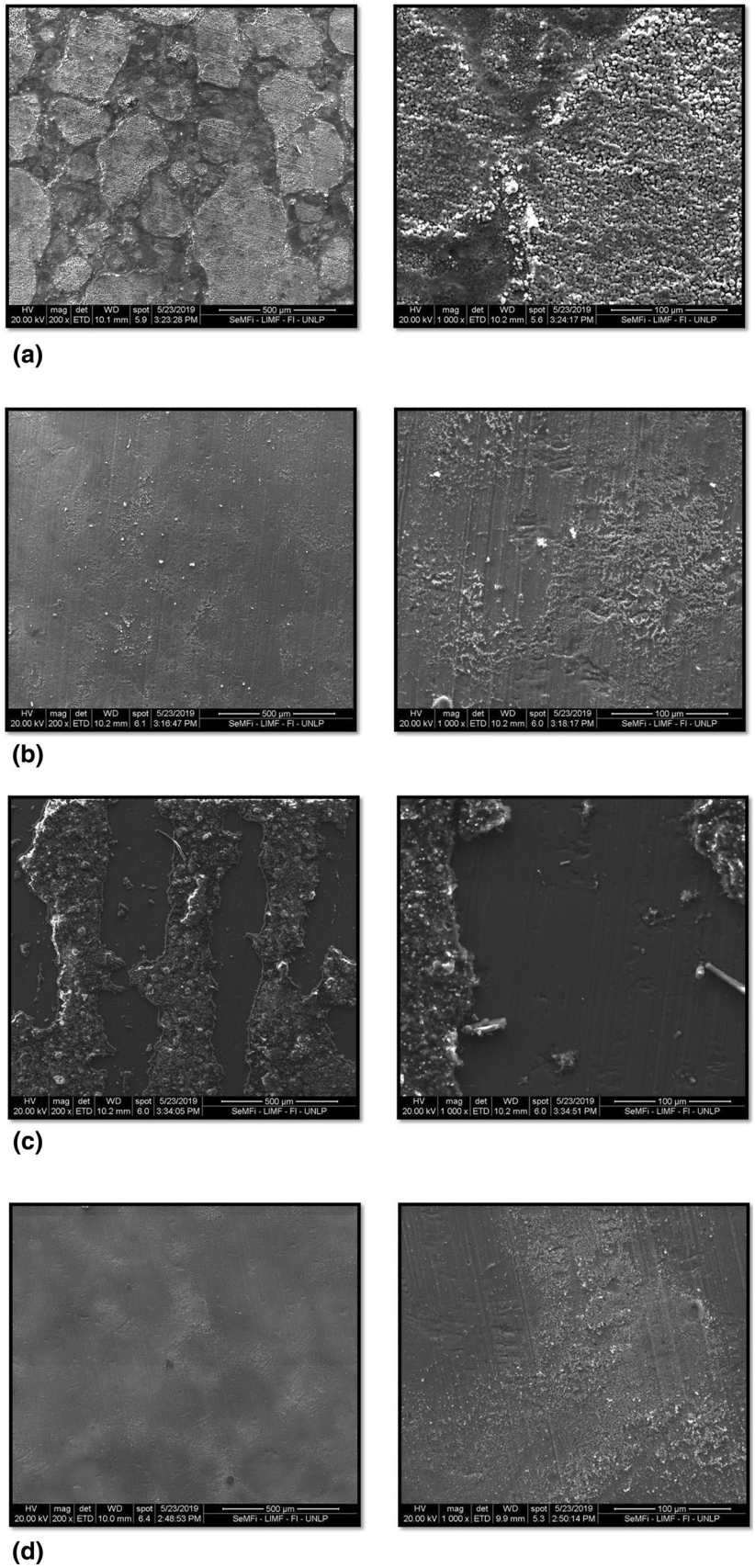

Fig. 12 SEM micrographs of (a) bare AA1050 substrate (blank coupons, B), and underlying substrate of (b) T40 coupons' underlying substrate, (c) CR coupons', (d) TAL coupons' underlying substrate, after humidity chamber exposure: 200X (left) and 1000X (right)

sive and eco-friendly alternative to chromates in the formulation of wash-primers for the temporary protection of aluminum.

Acknowledgments

The authors are grateful to CONICET (Consejo Nacional de Investigaciones Científicas y Técnicas), UNLP (Universidad Nacional de La Plata) and CICPBA (Comisión de Investigaciones Científicas de la Provincia de Buenos Aires) for their sponsorship to do this research.

References

1. A. Musa (2012) Corrosion Protection of Al Alloys Organic Coatings and Inhibitors, In: R. Shoja Razavi (Eds.) Recent Resear. Corr. Evaluat. Protect., 1st ed., IntechOpen, (2012), p. 51-68
2. C. Vargel, Introduction to the corrosion of aluminium, *Corrosion of aluminium*, 1st ed., C. Vargel Ed., Elsevier, 2004, p 81–109
3. L. Tomcsányi, K. Varga, I. Bartik, H. Horányi and E. Maleczki, Electrochemical Study of the Pitting Corrosion of Aluminium and its Alloys—II. Study of the Interaction of Chloride Ions with a Passive Film on Aluminium and Initiation of Pitting Corrosion, *Electrochim. Acta*, 1989, **34**(6), p 855–859
4. J. Soltis, Passivity Breakdown, Pit Initiation and Propagation of Pits in Metallic Materials – Review, *Corros. Sci.*, 2015, **90**, p 5–22
5. A. Carreira, A. Pereira, E. Vaz, A.M. Cabral, T. Ghidini, L. Pigliaru and T. Rohr, Alternative Corrosion Protection Pretreatments for Aluminum Alloys, *J. Coat. Technol. Res.*, 2017, **14**(4), p 879–892
6. J. Carlos de Haro, L. Magagnin, S. Turri and G. Griffini, Lignin-Based Anticorrosion Coatings for the Protection of Aluminum Surfaces, *ACS Sustain. Chem. Eng.*, 2019, **7**(6), p 6213–6222
7. H. Hlushko, Y. Cubides, R. Hlushko, T.M. Kelly, H. Castaneda and S.A. Sukhishvili, Hydrophobic Antioxidant Polymers for Corrosion Protection of an Aluminum Alloy, *ACS Sustain. Chem. Eng.*, 2018, **6**(11), p 14302–14313
8. S. Paul, Surface preparation and paint application,In: Surface Coatings. Science and Technology, 2 edition, Wiley, (1996), p. 477−510
9. J.M. Waldie, Conversion coatings, *Surface coatings paints and their applications*, 2nd ed., J.M. Waldie Ed., Springer Netherlands, 1984, p 578–588
10. E.W. Beale, Temporary protectives, *Corrosion*, 2nd ed., L.L. Shreir Ed., Newnes- Butterworths, 1976, p 17:21-17:29
11. M. Kendig, S. Jeanjaquet, R. Addison and J. Waldrop, Role of Hexavalent Chromium in the Inhibition of Corrosion of Aluminum Alloys, *Surf. Coat. Technol.*, 2001, **140**, p 58–66
12. R.L. Twite and G.P. Bierwagen, Review of Alternatives to Chromate for Corrosion Protection of Aluminum Aerospace Alloys, *Progr. Org. Coat.*, 1998, **33**(2), p 91–100
13. K. Xhanari and M. Finšgar, Organic Corrosion Inhibitors for Aluminum and its Alloys in Chloride and Alkaline Solutions: A Review, *Arab. J. Chem.*, 2019, **12**(8), p 4646–4663
14. A. Pizzi, Tannins: Prospectives and Actual Industrial Applications, *Biomolecules*, 2019, **9**(8), p 344–373
15. Y. Shirmohammadli, D. Efhamisisi and A. Pizzi, Tannins as a Sustainable Raw Material for Green Chemistry: A Review, *Ind. Crops Prod.*, 2018, **126**, p 316–332
16. A.K. Das, M.N. Islam, M.O. Faruk, M. Ashaduzzaman and R. Dungani, Review on Tannins: Extraction Processes, Applications and Possibilities, *S. Afr. J. Bot.*, 2020, **135**, p 58–70
17. O. D'Alessandro, G.J. Selmi, C. Deyá, A. Di Sarli and R. Romagnoli, Formulation and Assessment of a Wash-Primer Containing Lanthanum "Tannate" for Steel Temporary Protection, *J. Mater. Eng. Perform.*, 2018, **27**, p 687–704
18. M.S. Noor Idora, L.K. Quen and H.S. Kang, Effect of Tannin From *Rhizophora apiculate* as Corrosion Inhibitor for Epoxy Paint on Mild Steel, *J. Phys. Conf. Series*, 2017, **890**, p 012062
19. A.A. Rahim, M.J. Kassim, E. Rocca and J. Steinmetz, Mangrove (*Rhizophora apiculata*) Tannins: An Eco-Friendly Rust Converter, *Corros. Eng Sci. Technol.*, 2011, **46**, p 425–431
20. A.A. Rahim, E. Rocca, J. Steinmetz, M.J. Kassim, R. Adnan and M.M. Sani Ibrahim, Mangrove tannins and their flavanoid monomers as alternative steel corrosion inhibitors in acidic medium, *Corros. Sci.*, 2007, **49**, p 402–417
21. S. Martinez and I. Štern, Inhibitory Mechanism of Low-Carbon Steel Corrosion by Mimosa Tannin in Sulphuric acid Solutions, *J. Appl. Electrochem.*, 2001, **31**, p 973–978
22. R. Silveira Peres, E. Cassel, C.A. Ferreira and D. Schermann Azambuja, Black Wattle Tannin as a Zinc Phosphating Coating Sealer, *Surf. Interface Anal.*, 2014, **46**, p 1–6
23. G. Matamala, W. Smeltzer and G. Droguett, Comparison of Steel Anticorrosive Protection Formulated with Natural Tannins Extracted from Acacia and From Pine Bark, *Corros. Sci.*, 2000, **42**(8), p 1351–1362
24. L.F. Montoya, D. Contreras, A.F. Jaramillo, C. Carrasco, K. Fernández, B. Schwederski, D. Rojas and M.F. Melendrez, Study of Anticorrosive Coatings Based on High and Low Molecular Weight Polyphenols Extracted from the Pine Radiata Bark, *Progr. Org. Coat.*, 2019, **127**, p 100–109
25. O.R. Pardini, J.I. Amalvy and A.R. Di Sarli, Formulation and Testing of a Waterborne Primer Containing Chestnut Tannin, *J. Coat. Technol.*, 2001, **73**, p 99–106
26. C. Byrne, O. D'Alessandro, G.J. Selmi, R. Romagnoli and C. Deyá, Primers Based on Tara and Quebracho Tannins for Poorly Prepared Steel Surfaces, *Progr. Org. Coat.*, 2019, **130**, p 244–250
27. O. D'Alessandro, G.J. Selmi, C. Deyá, A.R. Di Sarli and R. Romagnoli, Lanthanum Derivative from "Tara" Tannin for Steel Temporary Protection, *Ind. Eng. Chem. Res.*, 2018, **57**, p 3215–3226
28. S. Flores Merino, J.J. Caprari, L. Vasquez Torres, L. Figueroa Ramos and A.A. Hadzich Girola, Inhibitive Action of Tara Tannin in Rust Converter Formulation, *Anti-Corros. Methods Mater.*, 2017, **64**(2), p 136–147
29. A. Hadzich, S. Flores, J. Caprari and R. Romagnoli, Study of Zinc Tannates Prepared with Tara Powder (*Caesalpinia spinosa*) as Anticorrosive Pigments in Alkyd Paints and Wash Primer Formulations, *Progr. Org. Coat.*, 2018, **117**, p 35–46
30. B. Zhao, W. Han, W. Zhang and B. Shi, Corrosion Inhibition Performance of Tannins for Mild Steel in Hydrochloric Acid Solution, *Res. Chem. Intermed.*, 2018, **44**(1), p 407–423
31. L. Mancero, La Tara (*Caesalpinia spinosa*) en Perú, Bolivia y Ecuador. Análisis de la Cadena Productiva en la Región, ECOBONA (Programa Regional Para la Gestión Social de Ecosistemas Forestales Andinos), (2008)
32. C. Aouf, S. Benyahya, A. Esnouf, S. Caillol, B. Boutevin and H. Fulcrand, Tara tannins as phenolic precursors of thermosetting epoxy resins, *Eur. Polym. J.*, 2014, **55**, p 186–198
33. J.-C. Castell, C. Fabregat, S. Sorolla, M. Jorba, A. Bacartit and L. Ollé, *Caesalpinia spinosa* (tara): The Sustainable Source of Tannins, *J. AQEIC*, 2012, **63**(2), p 21–30
34. J.M. Garro Galvez, B. Riedl and A.H. Conner, Analytical Studies on Tara Tannins, *Holzforschung*, 1997, **51**, p 235–243
35. S. Giovando, A. Pizzi, H. Pasch and N. Pretorius, Structure and Oligomers Distribution of Commercial Tara (*Caesalpina spinosa*) Hydrolysable Tannin, *ProLigno*, 2013, **9**(1), p 22–31
36. C. Gaidau, D. Simion, M. Niculescu, G. Paun, M. Popescu, A. Bacardit and C. Casas, Tara Tannin Extract Improvement I. Extraction and Concentration Through Membranary Filtration Techniques, *Rev. Chimie (Bucarest, Rom)*, 2014, **65**(8), p 629–633
37. H. Gerengi, A. Jazdzewska and M. Kurtay, A Comprehensive Evaluation of Mimosa Extract as a Corrosion Inhibitor on AA6060 Alloy in Acid Rain Solution: Part I. Electrochemical AC Methods, *J. Adhes. Sci. Technol.*, 2015, **29**(1), p 36–48
38. L. Guedes, K. Bacca, N. Lopes and E. Costa, Tannin of Acacia Mearnsii as Green Corrosion Inhibitor for AA7075-T6 Aluminum Alloy in Acidic Medium, *Mater. Corros.*, 2019, **70**, p 1288–1297
39. J.V. Nardeli, C.S. Fugivara, M. Taryba, E.R.P. Pinto, M.F. Montemor and A.V. Benedetti, Tannin: A Natural Corrosion Inhibitor for Aluminum Alloys, *Progr. Org. Coat.*, 2019, **135**, p 368–381
40. S.R.S. Rodrigues, V. Dalmoro and J.H.Z. Santos, An Evaluation of Acacia Mearnsii Tannin as an Aluminum Corrosion Inhibitor in Acid, Alkaline, and Neutral Media, *Mater. Corros.*, 2020, **71**(7), p 1160–1174

41. S. Yahya, A.A. Rahim, A. Mohd Shah and R. Adnan, Inhibitive Behaviour of Corrosion of Aluminium Alloy in NaCl by Mangrove Tannin, *Sains Malays.*, 2011, **40**(9), p 953–957
42. N.J.N. Nnaji, C.O.B. Okoye, N.O. Obi-Egbedi, M.A. Ezeokonkwo and J.U. Ani, Spectroscopic Characterization of Red Onion Skin Tannin and it's Use as Alternative Aluminium Corrosion Inhibitor in Hydrochloric Acid Solutions, *Int. J. Electrochem. Sci.*, 2013, **8**, p 1735–1758
43. N.J.N. Nnaji, N.O. Obi-Egbedi and C.O.B. Okoye, Cashew Nut Testa Tannin: Assessing its Effects on the Corrosion of Aluminium in HCl, *Port. Electrochim. Acta*, 2014, **32**(2), p 157–182
44. C. Byrne, G.J. Selmi, O. D'Alessandro and C. Deyá, Study of the Anticorrosive Properties of "Quebracho Colorado" Extract and its Use in a Primer for Aluminum1050, *Progr. Org. Coat.*, 2020, **148**, p 105827
45. Tannins, https://www.silvateam.com/en/ (Accessed 6th August 2020)
46. M.I. Karyakina and E. Kuzmak, Protection by Organic Coatings: Criteria, Testing Methods and Modelling, *Progr. Org. Coat.*, 1990, **18**, p 325–388
47. G.W. Walter, A Critical Review of d.c. Electrochemical Tests for Painted Metals, *Corros. Sci.*, 1986, **26**, p 39–47
48. "Standard Practice for Testing Water Resistance of Coatings in 100% Relative Humidity", D 2247, ASTM, (2015)
49. "Standard practice for measuring adhesion by Tape test", D 3359, ASTM, (2009)
50. "Standard test method for evaluating degree of blistering of paints", D 714, ASTM, (2002)
51. J.R. Davis, *Corrosion of Aluminum and Aluminum Alloys*, 1st ed. ASM International, 1999
52. F. dos Santos Grasel, M. Flôres Ferrão and C.R. Wolf, Development of Methodology for Identification the Nature of the Polyphenolic Extracts by FTIR Associated with Multivariate Analysis, *Spectrochim. Acta Part A.*, 2016, **2016**(153), p 94–101
53. L. Falcão and M. Araújo, Vegetable Tannins Used in the Manufacture of Historic Leathers, *Molecules*, 2018, **23**(5), p 1081
54. A. Ricci, K.J. Olejar, G.P. Parpinello, P.A. Kilmartin and A. Versari, Application of Fourier Transform Infrared (FTIR) Spectroscopy in the characterization of tannins, *Appl. Spectrosc Rev.*, 2015, **50**(5), p 407–442
55. K. Mansouri, K. Ibrik, N. Bensalah and A. Abdel-Wahab, Anodic Dissolution of Pure Aluminum during Electrocoagulation Process: Influence of Supporting Electrolyte, Initial pH, and Current Density, *Ind. Eng. Chem. Res.*, 2011, **50**, p 13362–13372
56. B. Zaid, D. Saidi, A. Benzaid and S. Hadji, Effects of pH and Chloride Concentration on Pitting Corrosion of AA6061 Aluminum Alloy, *Corros. Sci.*, 2008, **50**(7), p 1841–1847
57. A. Aballe, M. Bethencourt, F.J. Botana, M.J. Cano and M. Marcos, Inhibition of the Corrosion Process of Alloy AA5083 (Al-Mg) in Seawater by Cerium Cations. An EIS Study, *Mater. Corros.*, 2001, **52**, p 344–350
58. M.R. Laamari, J. Benzakour, F. Berrekhis, A. Derja and D. Villemin, Adsorption and Corrosion Inhibition of Carbon Steel in Hydrochloric Acid Medium by Hexamethylenediamine Tetra(Methylene Phosphonic Acid), *Arab. J. Chem.*, 2016, **9**, p S245–S251
59. M.R. Adam, A.A. Rahim and A.M. Shah, Synergy Between Iodide Ions and Mangrove Tannins as Inhibitors of Mild Steel Corrosion, *Ann. For. Sci.*, 2015, **72**(1), p 9–15
60. M.R. Vinutha and T.V. Venkatesha, Review on Mechanistic Action of Inhibitors on Steel Corrosion in Acidic Media, *Port. Electrochim. Acta*, 2016, **34**(3), p 157–184
61. S. Yoneda and F. Nakatsubo, Effects of the Hydroxylation Patterns and Degrees of Polymerization of Condensed Tannins on their Metal-Chelating Capacity, *J. Wood Chem. Technol.*, 1998, **18**(2), p 193–205
62. L. Zhang, R. Liu, B.W. Gung, S. Tindall, J.M. Gonzalez, J.J. Halvorson and A.E. Hagerman, Polyphenol-Aluminum Complex Formation: Implications for Aluminum Tolerance in Plants, *J. Agric. Food Chem.*, 2016, **64**(15), p 3025–3033
63. R. Padash, G. Sajadi, A.H. Jafari, E. Jamalzadeh and A. Shokuhi Rad, Corrosion Control of Aluminum in solutions of NaCl, HCl and NaOH using 2,6-dimethylpyridine inhibitor: experimental and DFT insights, *Mater. Chem. Phys.*, 2020, **244**, p 122681
64. M. Taghavikish, N.K. Dutta and N.R. Choudhury, Emerging corrosion inhibitors for interfacial coating, *Coatings*, 2017, **7**(12), p 217–245
65. M. Oki, Performance of Tannin/Glycerol-Chromate Hybrid Conversion Coating on Aluminium, *J. Mater. Sci. Chem. Eng.*, 2015, **03**(07), p 1–6
66. I. Kartsonakis, E.P. Koumoulos and C.A. Charitidis, Advancement in Corrosion Resistance of AA 2024–T3 Through Sol-Gel Coatings Including Nanocontainers, *Manuf. Rev.*, 2017, **4**, p 2
67. T. Kosako, M. Nishida and Y. Kadoya, Detection of Initial Stage of Aluminum Corrosion in NaCl Solution Utilizing Surface Plasmon Resonance, *IEEE Sens. J.*, 2020, **20**(16), p 9091–9096
68. P. Natishan and W. O'Grady, Chloride Ion Interactions with Oxide-Covered Aluminum Leading to Pitting Corrosion: A Review, *J. Electrochem. Soc.*, 2014, **161**, p C421–C432
69. E.M. Sherif and S.M. Park, Effects of 1,4-Naphthoquinone on Aluminum Corrosion in 0.50 M Sodium Chloride Solutions, *Electrochim Acta*, 2006, **51**(7), p 1313–1321
70. E. McCafferty, Sequence of Steps in the Pitting of Aluminum by Chloride Ions, *Corros. Sci.*, 2003, **45**(7), p 1421–1438
71. T. Burleigh, Corrosion of Aluminum and Its Alloys, In: Handbook of Aluminum, Vol. 2, Alloy Production and Materials Manufacturing, 1st ed., G.E. Totten, D.S. MacKenzie, Eds., Taylor & Francis, (2003), p. 421-463
72. A.A. Rahim and J. Kassim, Recent Development of Vegetal Tannins in Corrosion Protection of Iron and Steel, *Recent Pat. Mater. Sci.*, 2008, **100**, p 223–231
73. N. Kumar, M.K. Manoj and M.K. Phani, Influence of Potential Scan Rate on Corrosion Behaviour of Heat Treated AA 7075 Alloy in Sulphuric Acid Solution, *Mater. Sci. Res. India*, 2018, **15**(1), p 91–99
74. X.L. Zhang, Z.H. Jiang, Z.P. Yao, Y. Song and Z.D. Wu, Effects of Scan Rate on the Potentiodynamic Polarization Curve Obtained to Determine the Tafel Slopes and Corrosion Current Density, *Corros. Sci.*, 2009, **51**(3), p 581–587